

Atf İçin: Deniz A, 2021. Cr/Indigo Carmine/p-Si/Al Heteroeklem Diyotunun I-V-T Karakteristiklerinin İncelenmesi. İğdır Üniversitesi Fen Bilimleri Enstitüsü Dergisi, 11(4): 2790-2802.

To Cite: Deniz A, 2021. Investigation of I-V-T Charactersitics of Cr/Indigo Carmine/p-Si/Al Heterojunction Diode. Institute of Science and Technology, 11(4): 2790-2802.

Investigation of I-V-T Charactersitics of Cr/Indigo Carmine/p-Si/Al Heterojunction Diode

Ali Rıza DENİZ^{1*}

ABSTRACT: The subject of this study is the use of Indigo Carmine (IC) material in Schottky diode application. The *p*-Si crystal was chosen as the base material for diode fabrication. One surface of the *p*-Si metal was coated with Al metal by thermal evaporation method. Indigo carmine interface material was coated on the other surface of *p*-Si by spin coating method. Finally, Cr metal was coated on this material with DC sputtering method. So we obtained refence Cr/*p*-Si/Al diode and Cr/IC/*p*-Si/Al heterojunctions diode. When the current-voltage (*I*-*V*) measurements of these diodes at room temperature were examined, it was determined that the Indigo Carmine material improved the diode parameters. It was determined from the *I*-*V* measurements of the Cr/IC/*p*-Si/Al diode for different temperatures that the ideality factor (*n*) decreased and the barrier height (Φ_b) value increased with the increasing temperature. These changes with temperature have been attributed to the inhomogeneous distribution in the potential barrier. In addition, the change of diode parameters with temperature showed that the diode has a double Gaussian distribution.

Keywords: Indigo Carmine, Schottky diode, Thermionic Emission, Cheung, Norde, Current-Voltage.

¹Ali Rıza DENİZ ([Orcid ID: 0000-0003-3019-0522](https://orcid.org/0000-0003-3019-0522)), Hakkari Üniversitesi, Çölemerik MYO, Elektrik-Enerji Bölümü, Hakkari, Türkiye

*Sorumlu Yazar/Corresponding Author: Ali Rıza DENİZ, e-mail: alirizadeniz@hakkari.edu.tr

INTRODUCTION

Metal-semiconductor (MS) contacts take place in many areas in the developing electronics industry. Schottky diodes obtained from MS contacts in the electronics industry are used in many areas such as solar cells, microwave mixer detectors, varactors (capacitors whose capacities change with the applied voltage), fast switch applications (Balasubramani et al., 2020).

Schottky barrier height is the most important parameter for Schottky diodes. For this reason, many studies are carried out to increase the potential barrier. There are many studies in the literature on coating with various types of interface layers between metal and semiconductors (Reddy et al., 2020).

The use of polymers as metals and semiconductors accelerates the studies on this subject day by day. Conductive polymers are easy to prepare, easy to shape, cost effective, flexible materials. It is used in many fields due to its electrical, mechanical and physical properties. For example; Schottky diodes, fast switch applications, sensors, FETs, MESFETs, microwave circuit elements, solar cells, plastic batteries, varactors, electroluminescence devices (Güzel and Çolak, 2021).

Conjugated polymers are important for the production of solid state circuit elements. The fact that conjugated polymers have different groups in the molecular structure indicates that these polymers will cease to be an insulating material by chemical and electrochemical methods and gain metallic properties (Lim et al., 2016). In Schottky contacts made using conductive polymers, the barrier height increases while the ideality factor decreases as the temperature increases. This behavior indicates that the barrier heights at the interface have a Gaussian distribution, which means that there is no homogeneous distribution at the interface (Altan et al., 2020).

In this study, Indigo Carmine (IC) material was used as the interface material. This material is an organic salt soluble in water. IC is used as a colorant in foods, cosmetics and clothing. It is also used in medical applications. The IC material is produced by natural indigo sulfonation or fusion of N-phenylglycine in a mixture of sodamide and sodium and potassium hydroxide under ammonia pressure (Guaraldo et al., 2011; Kekes et al., 2020). IC molecules act as good electron acceptors. Due to its good electron acceptance properties, electron transfer processes take place under both intramolecular and intermolecular conditions. This material consists of donor-acceptor-donor electron groups, which provides remarkable electrical and optical properties (Pramodini and Poornesh, 2014).

Electrical measurements taken on Schottky diodes at different temperatures give a lot of information about diode parameters. Therefore, *I-V* measurements were taken at different temperature values for better understand the current transmission mechanism of the diode.

MATERIAL AND METHODS

Analyzing of The Indigo Carmine Material

The Indigo Carmine material was obtained from Sigma Aldrich Company. The molecular formula of this material is $C_{16}H_8N_2Na_2O_8S_2$ and its molecular weight is 466.35 g/mol. Fig. 1 shows the structural shape of indigo carmine material. The SEM image of IC is given in Fig. 2. The width of indigo carmine particles obtained from SEM images is around 5 ± 0.5 nm. As can be seen from the figure, these particles have a fine-sized dispersed structure and show a homogeneous distribution.

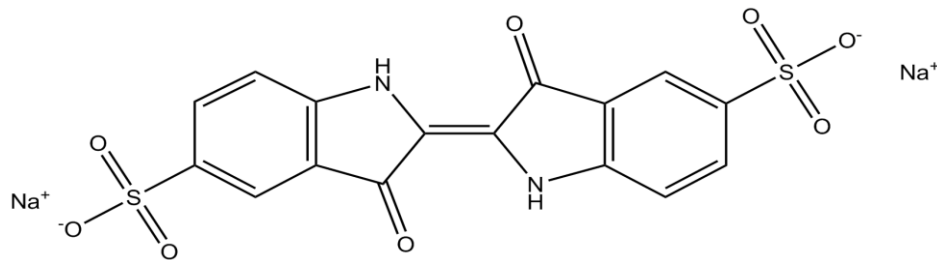


Figure 1. The schematic diagram of Indigo Carmine

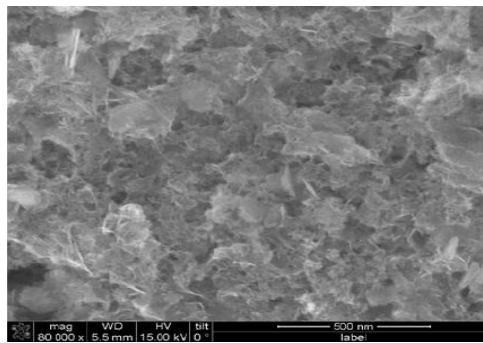


Figure 2. The SEM image of Indigo Carmine

Fabrication of The Diode

Chemical cleaning procedures RCA1 and RCA2 were applied to purify the *p*-Si crystal from surface impurities (Çaldıran, 2019). After the cleaning procedure, the matte side of the *p*-Si crystal was coated with Al metal using the thermal evaporation method. This sample was annealed at 580 °C for 3 minutes in N₂ atmosphere. Thus, Al/*p*-Si ohmic contacts were obtained. After the other surface of the *p*-Si crystal was coated with 10 nm thick IC material by spin coating method. Lastly, the Cr metal was coated on the indigo carmine material using the DC sputtering method. So, the reference Cr/*p*-Si/Al and Cr/IC/*p*-Si/Al diodes were obtained. The Fig. 3 shows the structural of Cr/IC/*p*-Si/Al diode.

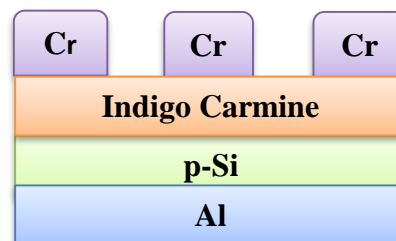


Figure 3. Schematic diagram of Cr/IC/*p*-Si/Al heterojunction

RESULTS AND DISCUSSION

The release of carriers from a hot surface due to their thermal energy is defined as thermionic emission. Electron transport through a potential barrier in Schottky contacts is explained by this theory.

According to the Thermionic Emission (TE) theory of a Schottky diode, the current in the case of forward bias is given by the following equation (1).

$$I = I_0 \left[\exp\left(\frac{eV}{nkT}\right) - 1 \right] \quad (1)$$

In this expression, if $eV \gg nkT$, "1" in the second term can be omitted. Thus, we obtain equation (2) by arranging equation (1).

$$I = I_0 \left[\exp\left(\frac{eV}{nkT}\right) \right] \quad (2)$$

If we take the natural logarithm of both sides of the expression (2) and then derive its derivative with respect to V , we get equation (3).

$$n = \frac{e}{kT} \frac{dV}{d(\ln I)} \quad (3)$$

The n expression obtained from equation (3) represents the ideality factor. The n is very important in determining the diode characteristic and has no unit. For a diode to be ideal, $n = 1$ must be. As the n value takes values greater than 1, the diode starts to move away from the ideal (Tung, 1991).

The greater value of the n may be due to the potential drop in the interfacial layer, the presence of overcurrent and recombination current through the interfacial states between the semiconductor/insulator layers (Reddy, 2014).

When we plot the $\ln I$ versus V from the I - V measurements of the diodes, a line is obtained if a fit is drawn towards the linear region in the line of supply. The $dV/d(\ln I)$ term is obtained from the slope of this line. The point where the line obtained from the drawn fit intersects the vertical axis at $V=0$ gives the saturation current density of I_0 .

$$I_0 = AA^*T^2 \exp\left(-\frac{e\Phi_b}{kT}\right) \quad (4)$$

In equation (4), if we take the natural logarithm of the terms and remove $e\Phi_b$ from the equation, we reach the equation that gives the Φ_b . This expression is calculated by equation (5).

$$e\Phi_b = kT \ln(AA^*T^2/I_0) \quad (5)$$

In the expression (5), A is the effective area of the diode ($A=0.00785 \text{ cm}^2$) A^* is the Richardson constant, and this value is $32 \text{ A K}^{-2} \text{ cm}^{-2}$ for p -Si (Rhoderich and Williams, 1988).

The I - V measurements of Cr/ p -Si/Al and Cr/IC/ p -Si/Al diodes were taken at room temperature. The **Fig.4** shows I - V graphs of these diodes. Also, the n and Φ_b values calculated and they are given in **Table 1**.

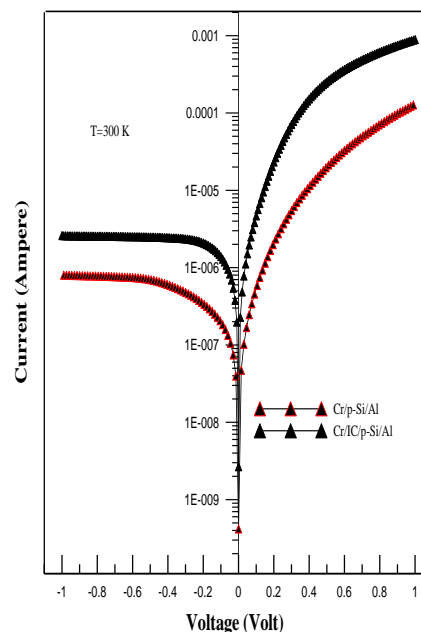


Figure4. The I - V graphs of Cr/ p -Si/Al and Cr/IC/ p -Si/Al diodes

Table 1. The n and Φ_b values of Cr/ p -Si/Al and Cr/IC/ p -Si/Al diodes

	n	Φ_b (eV)
Cr/ p -Si/Al	1.71	0.57
Cr/IC/ p -Si/Al	1.23	0.73

As can be seen from the calculated values of basic diode parameters, Indigo Carmine material made improvements in the electrical properties of the diode and contributed to the electrical conductivity of the diode. If it is considered that n value is 1 in ideal diodes, the n has decreased from 1.71 to 1.23. In addition, the Φ_b value in diodes has increased from 0.57 eV to 0.73 eV as desired. This indicates that the IC material is an electrically conductive material. IC material is frequently used in device construction due to its electrical conductivity, good film forming property and high thermal stability (Manthrammel et al., 2019).

The temperature dependent I - V graphs of the Cr/IC/p-Si/Al diode is given in **Fig. 4**. In addition, **Table 2** contains the n and Φ_b values of diode for temperature values between 120 K and 320 K ($\Delta T=20$ K).

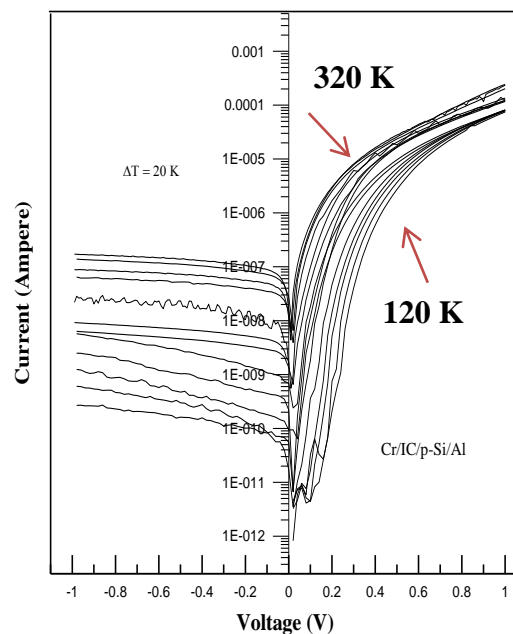


Figure 4. The I - V graphs of the Cr/IC/p-Si/Al diodes depending on temperature

Table 2. The n and Φ_b values of Cr/IC/p-Si/Al diode

Temperature (K)	n	Φ_b (eV)
120	2.08	0.27
140	1.97	0.30
160	1.85	0.37
180	1.76	0.43
200	1.67	0.52
220	1.52	0.56
240	1.44	0.61
260	1.36	0.66
280	1.29	0.69
300	1.23	0.73
320	1.21	0.75

The n - T and Φ_b - T graphs of the Cr/IC/p-Si/Al diode are given in **Figure 5**. When this graph is examined, as the temperature value increases, the n value decreases while the Φ_b value increases. It can also be observed in this graph that the I - V characteristic of the diode is strongly temperature dependent. Due to the inhomogeneous nature of the potential barrier at the MS interface, electrons pass through a low barrier at low temperatures, while at high temperatures they have the energy to cross a higher barrier. Thus, deviations from linearity occur in the I - V characteristic of the diode and the value

of the n increases (Afandiyeva et al., 2013). Also, the increase and decrease in the value of the n and Φ_b with the temperature change can be explained by the increase in inhomogeneity due to physical conditions such as surface defects, high density of interfacial state and non-homogenous doping concentration (Tung, 1992).

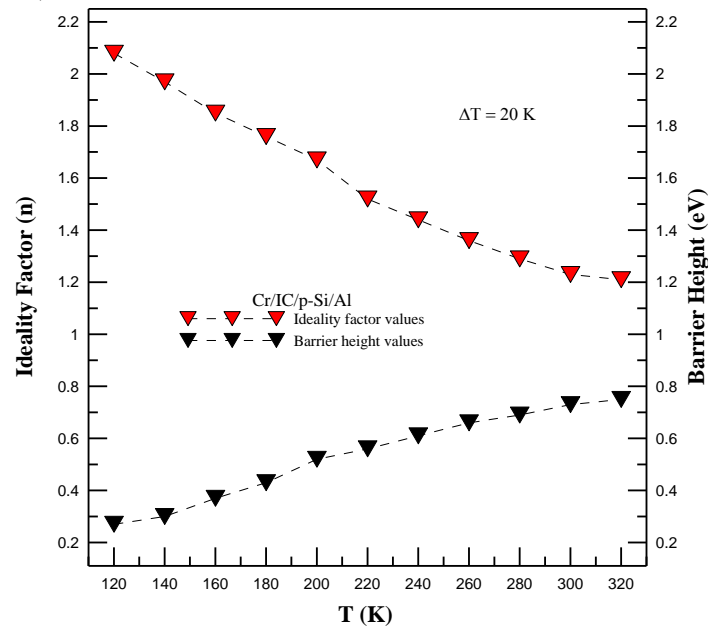


Figure 5. The n - T and Φ_b - T graphs of the Cr/IC/p-Si/Al diode

It is very important to calculate the series resistance R_s value of the diode in order to better analyze the deviations from linearity in the I - V characteristics of the diodes. The high R_s values adversely affect the electrical properties of diodes (Reddy et al., 2020). Cheung functions are the one of the most important ways to calculate the R_s value in diodes. Using the Cheung functions, we can also determine n and Φ_b values. Cheung functions are given by the following equations; (Werner and Gütter, 1991)

$$I = I_0 \exp \left[\frac{q(V - IR_s)}{nkT} \right] \tag{6}$$

$$\frac{dV}{d(\ln I)} = \frac{nkT}{q} + IR_s \tag{7}$$

$$H(I) = V - \left(\frac{nkT}{q} \right) \ln \left(\frac{I}{AA^*T^2} \right) \tag{8}$$

$$H(I) = n\Phi_b + IR_s \tag{9}$$

The $dV/d\ln I - I$ and $H(I) - I$ graphics of Cr/IC/p-Si/Al diode is given respectively **Fig. 6** and **Fig. 7**. The R_s and n values of the diode were calculated using Equation (6-7), the Φ_b and R_s values of the diode were calculated from equation (8-9). The n , Φ_b and R_s values of diode are given in **Table 3**. According to this table, the Φ_b values calculated from Cheung and TE models are close to each other. In **Fig. 8**, comparison of the n values calculated by Cheung and TE method depending on the temperature is given. According to this figure the value of n calculated from the Cheung method is greater than the value calculated by the TE method. This difference between values is attributed to the series resistance effect, interface states, and voltage drop across the interface layer (Hamdaoui et al., 2014).

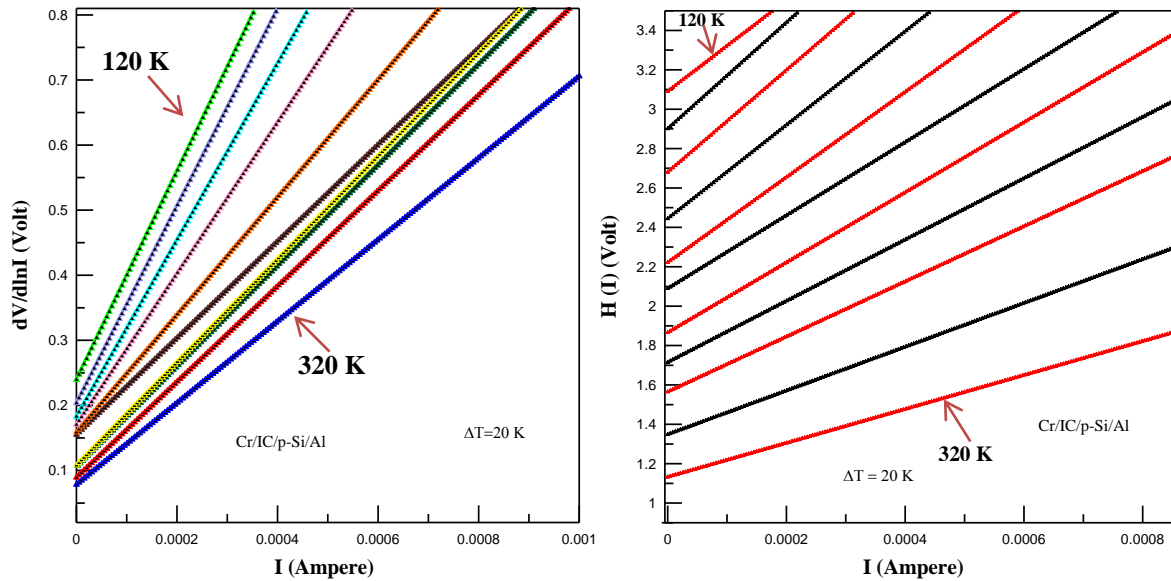


Figure 6. The $dV/d\ln I - I$ graphs of Cr/IC/p-Si/Al diode Figure 7. The $H(I) - I$ graphs of Cr/IC/p-Si/Al diode

Table 3. Basic diode parameters obtained using Cheung functions for Cr/IC/p-Si/Al diode

Temperature (K)	$dV/d\ln(I)$		$H(I)-I$	
	n	$R_s(\Omega)$	$\Phi_b(eV)$	$R_s(\Omega)$
120	4.57	5011	0.11	4565
140	4.21	4659	0.14	4016
160	3.65	4258	0.17	3755
180	3.27	3884	0.22	3304
200	2.98	3291	0.27	2999
220	2.56	2958	0.39	2690
240	2.27	2614	0.46	2388
260	2.02	2257	0.51	2001
280	1.89	2027	0.57	1846
300	1.71	1908	0.64	1733
320	1.57	1645	0.68	1385

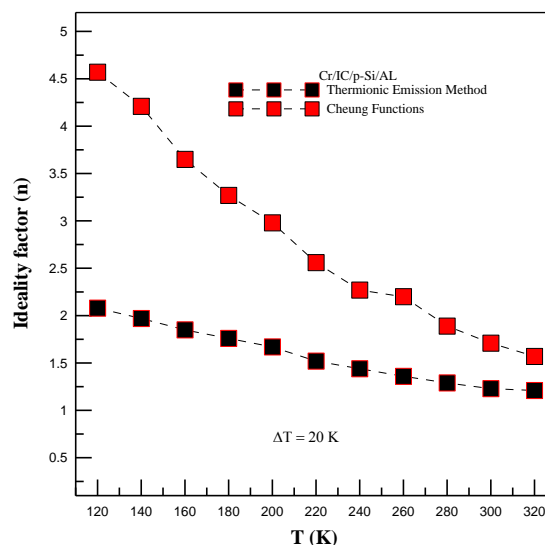


Figure 8 The comparison of n values calculated from Cheung and TE methods for Cr/IC/p-Si/Al diode

The Fig. 9 shows the temperature change graphs of the series resistance values of the Cr/IC/p-Si/Al diode. The R_s values calculated using the $dV/d(\ln I) - I$ and $H(I) - I$ curves of the diode are compatible with each other. As the temperature values increase, R_s values decrease. The reason for this

is that as the temperature increases, the number of free carrier increases with the effect of ionization and therefore more current passes through the diode (Chand and Kumar, 1996).

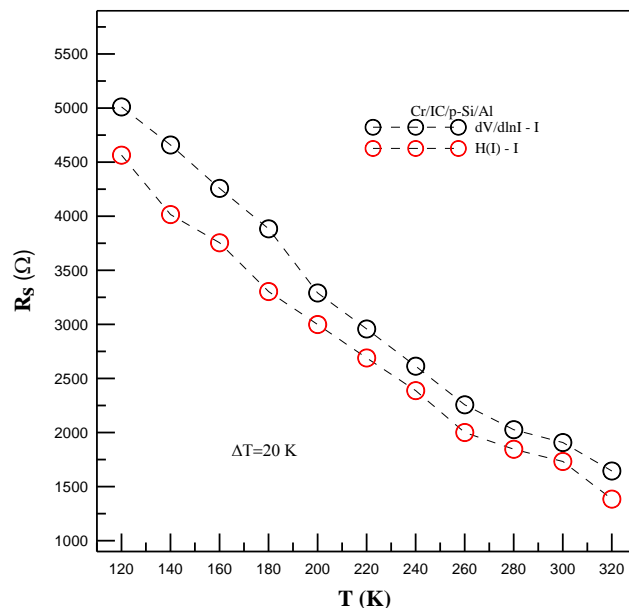


Figure 9. The $R_s - T$ graphs of Cr/IC/p-Si/Al diode (Cheung Functions)

The standard deviation and the σ_i has small value at high homogeneous barrier height gives important informations about the homogeneity of the potential barrier of diode. The σ_i value determines the size of the inhomogeneity in the barrier. For calculate the σ_i and the average barrier height $\overline{\Phi_b}$ values , we use the equation (10), which is the single Gaussian equation, is used.

$$\Phi_b = \Phi_{b1} - \frac{q\sigma_i^2}{2kT} \tag{10}$$

According to equation (10), the slope of the $\Phi_b - 1/T$ plot gives the σ_i standard deviation of the distribution and the point intersecting the y-axis gives the $\overline{\Phi_b}$ value at $V = 0$. The σ_i of a distribution determines the size of the distribution and indicates the effect and magnitude of potential barrier inhomogeneities in contact. The small σ_i and the $\overline{\Phi_b}$ value in a distribution means that the inhomogeneities present in the distribution are sufficiently small. The fact that σ_i has large values indicates that these anomalies in the contact structure are large and effective (Metin et al., 2014). One of the y-axes in **Fig. 10** shows the graphs of the $\Phi_b - 1/T$. **Fig. 10** shows that instead of a single intersecting linear line at 177 K, there are two linear lines at the MS interface, indicating the presence of two different barrier heights region. Therefore, the barrier at the MS interface shows a double Gaussian distribution (Beştaş et al., 2014). In order to calculate the voltage coefficients of the n values, the voltage coefficient of each distribution region is obtained using equation (11), which is the single Gaussian equation.

$$\left(\frac{1}{n_{ap}} - 1\right) = -\rho_2 + \frac{e\rho_3}{2kT} \tag{11}$$

The $[(1/n) - 1] - 1/T$ plot gives the voltage coefficient ρ_3 and ρ_2 of the distribution. Small voltage coefficients of ρ_3 and ρ_2 indicate that Schottky barrier inhomogeneities are small and if these coefficients are large, barrier inhomogeneities will be large (Ejderha et al., 2009). By applying the linear fit of the Φ_b values of the diode to two different distribution regions, the $\overline{\Phi_b}$ and σ_i values were calculated. These values are given in **Table 4**. Also, the other y-axis of **Fig. 10** shows the inverse of the n versus $q/2kT$. The n values have smaller values at high temperatures, while it is observed that the opposite of the n decreases more slowly at low temperatures due to the fact that the increase in the

values of the n is close to each other. Therefore, according to graph the values of the n show a double Gaussian distribution. The voltage coefficients from the plot of $(1/n) - I$ against $1/2kT$ are calculated and they are given in **Table 4**. The calculated σ_i values show that there is a large inhomogeneity in the diode interface. The inhomogeneous distribution at barrier height significantly affects the I - V characteristic of the diode (Bobby et al., 2013).

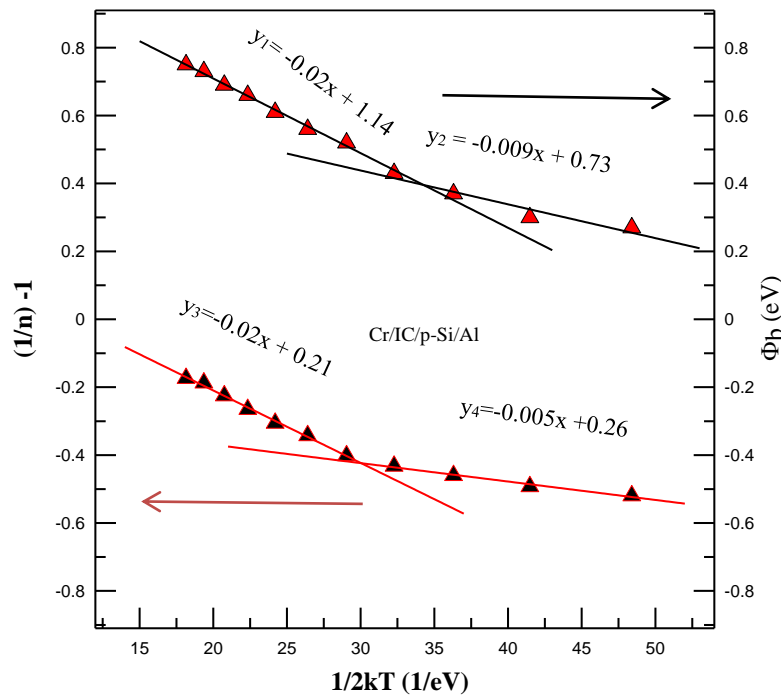


Figure 10. The $[(1/n) - I] - 1/2kT$ and $\Phi_b - 1/2kT$ graphs of Cr/IC/p-Si/Al diode

Table 4. The $\overline{\Phi_b}$, σ_i and voltage coefficients values of Cr/IC/p-Si/Al diode

T (K)	$\overline{\Phi_b}$ (eV)	σ_i	ρ_2	ρ_3
120 K -177 K	0.73	-0.009	-0.005	0.26
177 K -320 K	1.14	-0.02	-0.02	0.21

The effective Richardson constant A^* of the semiconductor surface is an important parameter in calculating the Schottky barrier height in MS contacts. Therefore, the calculation of the A^* constant is very important. Modified Richardson equation that can explain single distributions and is well known in the literature;

$$\ln\left(\frac{I_0}{T^2}\right) - \left(\frac{e^2\sigma_0^2}{2kT^2}\right) = \ln(AA^*) - \frac{e\overline{\Phi_b}}{kT} \tag{12}$$

The $\ln(I_0/T^2) - 1/T$ modified Richardson graph of Cr/IC/p-Si/Al diode is given in **Fig. 11**. The point intersecting the y-axis of the linear fit plotted on the modified Richardson graph gives the modified Richardson constant. The value of A^* calculated by using the slope of the line was determined as $A^* = 7.81 \text{ A K}^{-2} \text{ cm}^{-2}$. These experimentally obtained values are much less than $32 \text{ A K}^{-2} \text{ cm}^{-2}$ for the theoretically calculated p-Si. This is due to the inhomogeneous nature of the potential barrier. Due to the formation of oxide layers of different thickness between the metal and semiconductor, high and low barrier patches occur at the interface. Due to these potential fluctuations at the contact interface, the diode current prefers low barriers in potential distribution (Sharma and Periasamy, 2014).

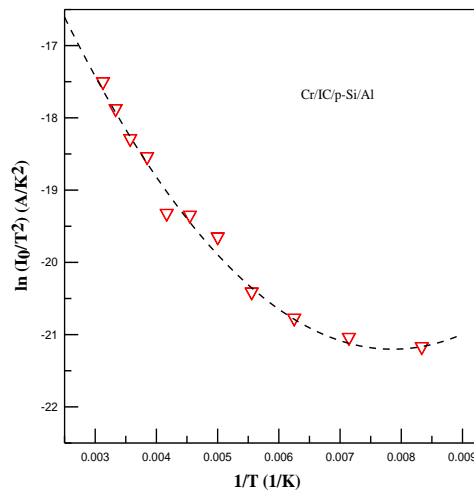


Figure 11. Modified Richardson plot of Cr/IC/p-Si/Al diode

New methods have been developed to determine physical (electronic) parameters such as R_s , n and Φ_b in MS contacts. One of these is the $F(V)$ function, which is defined by Norde for the R_s and Φ_b for $n = 1$ (Norde, 1979). This function is given by the following equation.

$$F(V) = \frac{V}{\gamma} - \left(\frac{kT}{2}\right) \ln\left(\frac{I(V)}{AA^*T^2}\right) \tag{13}$$

The $I(V)$ expression in equation (13) is the current value obtained from the $I-V$ graph of the diode, and γ is a random integer greater than the n value. First, the graph of F versus V is plotted. From this graph, the minimum value of $F(V)$ against V is determined. With the help of this equation, the Φ_b value is calculated by equation (14).

$$\Phi_b = F(V_0) + \frac{V_0}{\gamma} - \frac{kT}{q} \tag{14}$$

The value of $F(V_0)$ in this equation is the minimum value of $F(V)$ and V_0 is the minimum value corresponding to this value. R_s values are calculated by equation (15) (Zhang et al., 2013).

$$R_s = \frac{kT(\gamma-n)}{qI_0} \tag{15}$$

The Fig. 12 shows the $F(V) - V$ graphs of Cr/IC/p-Si/Al diode. Table 5 contains the Φ_b and R_s values of diode which are calculated with Norde functions.

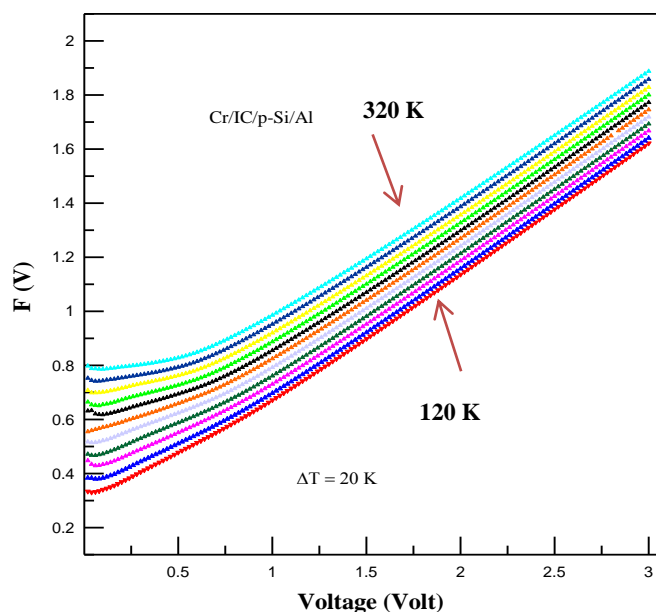
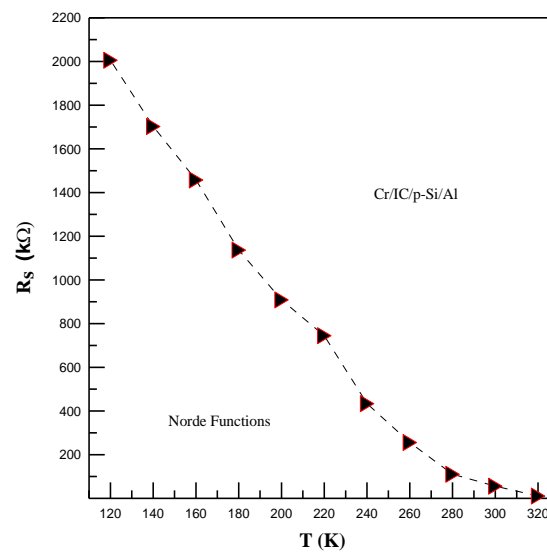


Figure 12. The $F(V) - V$ plots of Cr/IC/p-Si/Al diode

Table 5. The Φ_b and R_s values of Cr/IC/p-Si/Al diode (Norde functions)

Temperature (K)	Φ_b (eV)	R_s (k Ω)
120	0.21	2006
140	0.26	1703
160	0.30	1458
180	0.38	1137
200	0.41	909
220	0.46	745
240	0.53	434
260	0.57	256
280	0.62	111
300	0.68	56.3
320	0.73	11.2

**Figure 13.** The R_s – T graph of Cr/IC/p-Si/Al diode (Norde Functions)

The values of Φ_b calculated using the Norde functions are almost the same as the values calculated from the TE and Cheung methods. It also shows a harmonious change in temperature. **Fig. 13** shows the temperature-dependent change graph of the R_s values calculated from the Norde functions for Cr/IC/p-Si/Al diode. According to this graph, the R_s values decreases with increasing temperature. The reason for this change is that the free carrier concentration increases as the temperature increases (Sağlam et al., 2013; Deniz et al., 2014).

CONCLUSIONS

In this study, room temperature I - V measurements of Cr/p-Si/Al and Cr/IC/p-Si/Al diodes which are fabricated under the same conditions were analyzed and it was determined that the Indigo Carmine material caused an improvement in the basic diode parameters of the diode. This is due to the fact that the Indigo Carmine material is an electrically conductive material. From the temperature-dependent measurements of the Cr/IC/p-Si/Al diode, it was determined that the n value and the R_s value decreased with increasing temperature, while the Φ_b value increased. The effective Richardson constant of the diode was determined as $A^* = 7.81 \text{ A K}^{-2}\text{cm}^{-2}$. These experimentally obtained values are much less than $32 \text{ A/K}^2\text{cm}^2$ for p-Si calculated theoretically. This is due to the inhomogeneous nature of the potential barrier. In addition, it has been determined that the potential barrier at the contact interface has a double Gaussian distribution.

Conflict of Interest

The article was written by a single author. All studies in the article were carried out by assistant professor Dr Ali Rıza DENİZ.

Author's Contributions

Since the article is written by a single author, there is no conflict of interest.

REFERENCES

- Afandiyeva IM, Demirezen S, Altındal Ş, 2013. Temperature dependence of forward and reverse bias current-voltage characteristics in Al-TiW-PtSi/*n*-Si Schottky barrier diodes with the amorphous diffusion barrier. *Journal of Alloys and Compounds*, 552:423-429.
- Altan H, Özer M, Ezgin H, 2020. Investigation of electrical parameters of Au/P3HT:PCBM/ *n*-6H-SiC/Ag Schottky barrier diode with different current conduction models. *Superlattices and Microstructures*, 146:106658.
- Balasubramani V, Chandrasekaran J, Nyugen TD, Maruthamuthu S, Marnadu R, Vivek P, Sugarthi S, 2020. Colossal photosensitive boost in Schottky diode behaviour with Ce-V₂O₅ interfaced layer of MIS structure. *Sensors and Actuators A: Physical*, 315:112333.
- Beştaş AN, Yazıcı S, Aktaş F, Abay B, 2014. Double Gaussian distribution of barrier height for FeCrNiC alloy Schottky contacts on *p*-Si substrates. *Applied Surface Science*, 318:280-284.
- Bobby A, Verma S, Asokan K, Sarun PM, Antony BK, 2013. Phase transition induced double-Gaussian barrier height distribution in Schottky diode. *Physica B*, 431:6-10.
- Chand S, Kumar J, 1996. Evidence for the double distribution of barrier heights in Pd₂Si/*n*-Si Schottky diodes from *I-V-T* measurements. *Semiconductor Science and Technology*, 11(1):1203-1208.
- Çaldıran Z, 2019. Fabrication of Schottky barrier diodes with the lithium fluoride interface layer and electrical characterization in a wide temperature range. *Journal of Alloys and Compounds*, 816:152601.
- Deniz AR, Çaldıran Z, Metin Ö, Can H, Meral K, Aydoğan Ş, 2014. Schottky diode performance of an Au/Pd/GaAs device fabricated by deposition of monodisperse palladium nanoparticles over a *p*-type GaAs substrate. *Materials Science in Semiconductor Processing*, 27:163-169.
- Ejderha K, Yıldırım N, Abay B, Turut A, 2009. Examination by interfacial layer and inhomogeneous barrier height model of temperature-dependent *I-V* characteristics in Co/*p*-InP contacts. *Journal of Alloys and Compounds*, 484:870-876.
- Guaraldo TT, Pulcinelli SH, Zanoni MVB, 2011. Influence of particle size on the photoactivity of Ti/TiO₂ thin film electrodes, and enhanced photoelectro catalytic degradation of indigo carmine dye. *Journal of Photochemistry and Photobiology A:Chemistry*, 217:259-266.
- Güzel T, Çolak AB, 2021. Artificial intelligence approach on predicting current values of polymer interface Schottky diode based on temperature and voltage: An experimental study. *Superlattices and Microstructures*, 153:106864.
- Hamdaoui N, Ajjel R, Salem B, Gendry M, 2014. Distribution of barrier heights in metal/*n*-InAlAs Schottky diodes from current-voltage-temperature measurements. *Materials Science in Semiconductor Processing*, 26:431-437.
- Kekes T, Tzia C, 2020. Adsorption of indigo carmine on functional chitosan and β-cyclodextrin/chitosan beads: Equilibrium, kinetics and mechanism studies. *Journal of Environmental Management*, 262:110372.
- Lim LW, Aziz F, Muhammad FF, Supangat A, Sulaiman K, 2016. Electrical properties of Al/PTB7-Th/*n*-Si metal-polymer-semiconductor Schottky barrier diode. *Synthetic Metals*, 221:169-175.

- Manthrammel MA, Yahia IS, Shkir M, Alfaify S, Zahran HY, Ganesh V, Yakuphanoglu F, 2019. Novel design and microelectronic analysis of highly stable Au/Indigo/*n*-Si photodiode for optoelectronic applications, *Solid State Sciences*, 93:7-12.
- Metin Ö, Aydoğan Ş, Meral K, 2014. A new route for the synthesis of graphene oxide-Fe₃O₄ (GO-Fe₃O₄) nanocomposites and their Schottky diode applications. *Journal of Alloys and Compounds*, 585:681-688.
- Norde H, 1979. A modified forward *I-V* plot for Schottky diodes with high series resistance. *Journal of Applied Physics*, 7(50):5052.
- Pramodini S, Poornesh P, 2014. Third-order nonlinear optical response of indigo carmine under 633 nm excitation for nonlinear optical applications. *Optics & Laser Technology*, 63:114-119.
- Reddy PRS, Janardhanam V, Shim K-H, Lee S-N, Kumar AA, Reddy VR, Choi CJ, 2020. Temperature dependent Schottky barrier characteristics of Al/*n*-type Si Schottky barrier diode with Au-Cu phthalocyanine interlayer. *Thin Solid Films*, 713:138343.
- Reddy PRS, Janardhanam V, Shim K-H, Reddy VR, Lee S-N, Park S-J, Choi C-J, 2020. Temperature-dependent Schottky barrier parameters of Ni/Au on *n*-type (001) β-Ga₂O₃ Schottky barrier diode. *Vacuum*, 171:109012.
- Reddy VR, 2014. Electrical properties and conduction mechanism of an organic-modified Au/NiPc/*n*-InP Schottky barrier diode. *Applied Physics A*, 116:1379-1387.
- Rhoderick EH, Williams RH, 1988. *Metal semiconductor contacts*. 2nd ed. Oxford University Press.
- Sağlam M, Güzeldir B, Ateş A, Buğur E, 2013. Temperature dependence of current-voltage characteristics of the Cd/CdS/*n*-GaAs/In sandwich structure. *Journal of Physics and Chemistry of Solids*, 74:370-376.
- Sharma S, Periasamy C, 2014. A study on the electrical characteristic of *n*-ZnO/*p*-Si heterojunction diode prepared by vacuum coating technique. *Superlattices and Microstructures*, 73:12-21.
- Tung RT, 1991. Electron transport of inhomogeneous Schottky barriers. *Applied Physics Letter*, 83:2821-2823.
- Tung RT, 1992. Electron transport at metal-semiconductor interfaces. *General Theory Physical Review B*, 45:13509.
- Werner JH, Gütter HH, 1991. Barrier inhomogeneities at Schottky contacts. *Journal Applied Physics*, 69(3):1522-1532.
- Zhang X, Zhai J, Yu X, Ding L, Zhang W, 2013. Fabrication and characterization of flexible Ag/ZnO Schottky diodes on polyimide substrates. *Thin Solid Films*, 548:623-626.